Simulation of Fluid flow and Thermal Transport in Gravity-dominated Microchannel

[1]Isaac F. Odesola[2]Abimbola .Ashaju, [1]Ebenezer O. Ige.
[1]Department of Mechanical Engineering University of Ibadan, Ibadan NIGERIA
[2] Université PARIS-EST Marne-la-Vallée, 5 BvdDescartes,Champs-sur-Marne, F-77454 Marne-la-Vallée, France
E-mail: samuelashaju@gmail.com

Abstract— The success recorded by the usage of microchannel in high flux cooling application, has led to several studies aimed at advancement, in microchannel fluid flow and heat transfer technology. A recent study area with promising breakthrough is the effects of gravity on microscale flow. In this study, microchannels inclined at angles 0° 30° and 60° were investigated. Using the finite volume method, numerical computations were carried out on models which were coupled with the continuity equation, momentum and energy equations. With water as the working fluid, the fluid flow and heat transfer characteristics were evaluated in the form of the friction factor (*f*) and Nusselt number (Nu). Fluid flow was found to be highly optimized for microchannels of hydraulic diameter Dh=1587 μm, inclined at 30° and 60°. Heat transfer enhancement was obtained for microchannel (Dh=199 μm) inclined at 60°. This result illustrates the potential of microchannel angular orientation as a passive tool for flow optimization and heat enhancement.

Index Terms— Friction factor, Single Phase flow, Nusselt number, Inclination Angle, gravity flow

Nomenclature

	Channel cross-sectional area	$m2$
A		
A	Channel height	m
b	Channel width	M
C_p	Specific Heat capacity	$\frac{J}{Kg}.K$
Dh	Hydraulic diameter	m
E	east	
f	Friction factor	
H	Microchannel height	m
K	Thermal conductivity	W/m^2K
In	Inlet	
N	North	
P	Pressure	Pa
Re	Reynolds number	
S	Source term	
S	South	
T	Temperature	K
U	Velocity component	m/s
v	Average fluid velocity	m/s
W	west	

Greek symbols

α	Aspect ratio	
μ	Dynamic viscosity	$Kg/m.s$
ρ	Density	Kg/m^3
β	Proportionality factor	
Φ	Viscous dissipation	
ϕ	Transport variable	
Γ	Diffusion coefficient	

1. INTRODUCTION

Evolution in the design of electronic device and system, has led to the development of miniaturized system that consists of wider circuit integration for multifunctional purposes.The high performance associated with it, has brought about high heat flux generation and heat management issues which poses a great challenge to thermal and fluid engineers. There is a growing need to design miniature cooling systems that would not only conform to the design considerations, but would also guarantee high heat flux dissipation, and this has birthed the advent of microchannel. A micro-channel is a medium through which fluid is used to dissipate heat from a hot surface by forcing the fluid through a passage. Its hydraulic diameter ranges from 10μm to 200 μm.

Tukerman and Pease [1] pioneered the application of micro-channels as suitable heat sinks for electronic cooling.They were able to successfully dissipate high heat flux (as high as 800W/m^2), using micro-channels.This major milestone has opened the door for future research in the field of microscale flow and heat transfer.

Fluid flow and heat transfer in microchannel has been found to be influenced by Microchannel configuration,

geometry, and aspect ratio [2].Pega and Xiao [3]investigated rectangular microchannel with hydraulic diameter (69.5μm - 304.7μm), and aspect ratios (0.09 to 0.24) using R134a as the working fluid. They concluded that, in the laminar region, the experimental values for frictional constant $\boldsymbol{f.Re}$for R134a, in four microchannel with smoother surfaces [$\frac{R_a}{Dh} < 0.3\%$]agree with analytical solution based on the Navier-stokes equation.

Omar et al. [4] investigated an experimental microchannel characterized by a rectangular cross-section and large aspect ratio by varying the hydraulic diameter of the microchannel, they reported that the conventional laws and correlations that describe the flow in ducts of large dimension can be applied directly to microchannel, whose height ranges between 500 and 50 microns. Wu and Cheng [5] obtained a correlation between the Poiseuille number, and aspect ratio, in a trapezoidal silicon microchannel, they observed that the friction constant of the microchannel is greatly influenced by the cross-sectional aspect ratio, Wb/Wt.

Several works has been carried out to determine the nature of microchannel heat transfer [6], [7], [8], [9], [10], [11]. Over the last decade, convective heat transfer in microchannels has gravitated towards the application of nanofluid as working fluid, these works have showcased the potential of nanofluid in terms of higher thermal conductivity which can largely enhance greatly heat transfer. Some authors [12] [13] [14] [15] reported the enhancement of the heat transfer coefficient for nanofluid convective flow, citing several factors such as Peclet number, particle size, shape and volume fraction as being responsible for this enhancement.

A comprehensive review on the different methodologies and correlations used in predicting the heat transfer and pressure drop characteristicsof microchannels along the channel geometries and flow regimes, using both experimental and numerical approaches can be found in [7].

Despite the advancements made with respect to aspect ratio on fluid flow, none has geared towards gravity dominated microscale flow. This study aims to investigate, the influence of gravity on the fluid flow and thermal characteristics for a microchannels inclined at two angles, 30° and 60°.The gravity force is expected to optimize fluid flow, reduce pressure drop, and enhance convective heat flow. This passive fluid flow control strategywould lead to newer design configurations for microfluidic systems.

2.0 PROBLEM FORMULATION

Fig.1 shows the schematic diagram of the microchannel inclined at angle θ, the inclinationangle accounts for varying gravity influence on the microchannel. We considered a fully developed, steady state laminar flow in a two dimensional channel with length (b) and width (a). The working fluid which in this case, water, is incompressible.

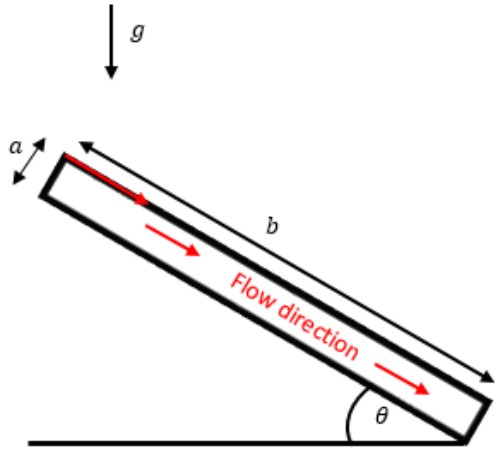

Fig. 1. Schematic of 2D rectangular microchannel

2.1 Governing equations and boundary conditions

The following equations govern the fluid flow and heat transfer, they include,continuity equation, Momentum equation for the Fluid flow, and the energy equation for the heat transfer process, which were modelled under steady state conditions.

Continuity equation

$$\frac{\partial u}{\partial x} + \frac{\partial v}{\partial y} = 0 \quad (1)$$

Momentum equation

- X-component of the Momentum equation

$$\rho\left[u\frac{\partial u}{\partial x} + v\frac{\partial u}{\partial y}\right] = -\frac{\partial p}{\partial x} + \mu\left[\frac{\partial^2 u}{\partial x^2} + \frac{\partial^2 u}{\partial y^2}\right] + f cos\theta \quad (2)$$

- Y-component of the Momentum equation

$$\rho\left[u\frac{\partial v}{\partial x} + v\frac{\partial v}{\partial y}\right] = -\frac{\partial p}{\partial y} + \mu\left[\frac{\partial^2 v}{\partial x^2} + \frac{\partial^2 v}{\partial y^2}\right] + f cos\theta \quad (3)$$

Energy equation

$$\rho C_p\left[u\frac{\partial T}{\partial x} + v\frac{\partial T}{\partial Y}\right] = k\left[\frac{\partial^2 T}{\partial x^2} + \frac{\partial^2 T}{\partial y^2}\right] \quad (4)$$

2.1.1 Gravity Vector $\bar{g}$

We consider the two dimensional laminar flow of a Newtonian fluid within a microchannel, inclined at angle $\theta > 0$, and a x, y coordinate system, with the x-axis along the inclination plane, and the y-axis at the horizontal axis normal to the inclination plane.

The gravity vector is resolved into two components as shown in Fig. 2. Firstly, resolution along the parallel plane gives, $F_g sin\theta$, and the perpendicular direction is $F_g cos\,\theta$.

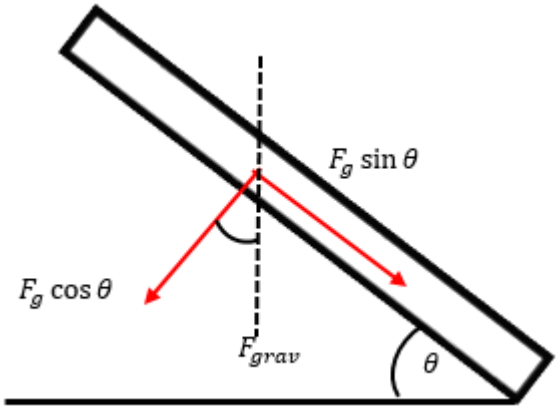

Fig. 2. Resolution of the gravity vector

The conservation equations was used to derive the gravity vector which is resolved into the horizontal and vertical component. Thefollowing assumptions together with expression (5), were applied to expressions (6) *and* (7)leading to (8)*and* (9)

- Steady state condition $\frac{\partial}{\partial t} = 0$
- Incompressible fluid $\frac{\partial \rho}{\partial x} = \frac{\partial \rho}{\partial y} = \frac{\partial \rho}{\partial z}$
- Flow is in the Y direction $v_x = 0$
- Viscous dissipation is negligible

Continuity Equation
For a Cartesian coordinate, the continuity equation is

$$\frac{\partial \rho}{\partial t} + \left[v_x \frac{\partial \rho}{\partial x} + v_y \frac{\partial \rho}{\partial y}\right] + \rho\left[\frac{\partial v_x}{\partial x} + \frac{\partial v_y}{\partial y}\right] = 0 \quad (5)$$

Momentum equation

$$\rho\left[\frac{\partial v_x}{\partial t} + v_x \frac{\partial v_x}{\partial x} + v_y \frac{\partial v_x}{\partial y}\right] = -\frac{\partial \rho}{\partial x} + \mu\left[\frac{\partial^2 v_x}{\partial x^2} + \frac{\partial^2 v_x}{\partial y^2}\right] + \rho g_x \quad (6)$$

$$\rho\left[\frac{\partial v_z}{\partial t} + v_x \frac{\partial v_z}{\partial x} + v_y \frac{\partial v_y}{\partial y}\right] = -\frac{\partial \rho}{\partial y} + \mu\left[\frac{\partial^2 v_y}{\partial x^2} + \frac{\partial^2 v_y}{\partial z^2}\right] + \rho g_y \quad (7)$$

$$0 = -\frac{\partial \rho}{\partial x} + \rho g_x \quad (8)$$

$$0 = -\frac{\partial \rho}{\partial z} + \mu\left[\frac{\partial^2 y}{\partial x^2}\right] + \rho g_y \quad (9)$$

Introduction of the gravity vector into the coordinate system gives the modified momentum equations which are:

X-component $0 = -\frac{\partial P}{\partial x} + \rho g sin\theta$ (10)

Y-component $0 = -\frac{\partial P}{\partial x} + \mu\left[\frac{\partial^2 v_y}{\partial x^2}\right] + \rho g cos\,\theta$ (11)

Since no pressure gradient was applied in driving the flow, the flow is then driven by gravity alone, therefore

X-component becomes $\frac{\partial P}{\partial x} = \rho g\, sin\,\theta$ (12)

Y-component becomes $\frac{\partial^2 v_y}{\partial x^2} = -\frac{\rho g}{\mu} cos\,\theta$ (13)

2.2 Boundary Condition

The no-slip boundary condition is imposed for the velocity components at the channel walls

$y = 0, \quad v = 0$

x = H, u=u_y

Inlet

The average velocity and Incoming fluid temperature is specified as:

y=0,$V = u_y = 0.116m/s, T = T_{in} = 293k$

Outlet

$\left[\frac{\partial V}{\partial y}\right] = 0$, $\left[\frac{\partial T}{\partial y}\right] = 0$

Top and Bottom wall

The heat flux at the top and bottom of the channel is defined as:

$$\begin{cases} x = 0\,, 0 \le y \le a \\ x = b\,, 0 \le y \le a \end{cases} q'' = -k\frac{\partial T}{\partial y} = 100000 \;\; W/m^2$$

We assumed zero interaction between the free surface and the ambient fluid above, because the working fluid is bounded within the microchannel, therefore we ignored the surface tension effects on the fluid surface.

3.0 NUMERICAL METHOD

We adopted the finite volume method as the computational approach, it involves the formulation of a control volume where the governing equations are linearized and integrated over each cell nodes. The flow and energy equations were transformed to a general convective diffusive transport equation shown in equation (14).

$$\nabla(\rho\phi\bar{V}) = \nabla\left(\Gamma_\phi \nabla\phi\right) + S_\phi \quad (14)$$

ϕ is the transport variable containing u, v and T

Γ_ϕ is the diffusion coefficient containing μ and K/C_p

S_ϕ is the source term containing $-\frac{\partial p}{\partial x}, -\frac{\partial p}{\partial y}, \rho g cos\theta$

S

$$\int_W^E \frac{d}{dx}(\rho u\phi) + \int_S^N \frac{d}{dy}(\rho u\phi) = \int_W^E \frac{d}{dx}\left(\Gamma \frac{d\phi}{dx}\right) + \int_S^N \frac{d}{dy}\left(\Gamma \frac{d\phi}{dy}\right) \quad (15)$$

The Finite volume method converts the partial differential equation into multiple series algebraic equation shown in (16), where the unknowns are the discrete nodal values.

$a_P\phi_P = a_W\phi_W + a_E\phi_E + a_S\phi_S + a_N\phi_N + b$ (16)

$b = S_c \Delta x \Delta y \Delta z$ (17)

$S_\phi = S_c + S_P\phi_P$ (18)

For the Spatial Discretization, the least square cells method was employed to determine the gradient of the variables at the cell faces, the second order upwind discretization scheme is used to compute momentum and energy quantities at cell faces using a multidimensional linear reconstruction approach through a Taylor series expansion of the cell-centered solution about the cell centroid.

3.1 Simulation

The working fluid adopted for this study was water, its thermo-physical properties at room temperature were obtained from the material database of FLUENT. The simulation parameters for the fluid flow and heat transfer corresponding to the boundary conditions are shown in Tables 1 and 2.
The simulations were initialized using Hybrid method which solves the Laplace equation to produce a velocity field and pressure field that smoothly connects high and low pressure values in the computational domain. Convergence criteria was set by ensuring that the residuals for all equations dropped below 10^{-12} , a velocity monitor introduced at the pressure outlet indicates the resolution of the continuity equation.

TABLE 1: Fluid flow conditions

Parameter	Value	Boundary conditions
Velocity m/s	As defined by Re	Inlet
Pressure (Pa)	0	Outlet
	No-slip	Wall
Gravity (N/m^2)	9.81	y-coordinate

TABLE 2: Heat transfer in Fluids Simulation Parameter

Parameter	Value	Boundary conditions
Velocity field (m/s)	Specified by Reynolds number	Inlet
Inlet temperature	293K	Entire domain of microchannel
Pressure Outflow	0 Pa	Outlet
Heat Flux	100000 W/m^2	Upper and lower planes of the microchannel

The micro-channels of smooth surfaces were inclined at angles of 0°, 30° and 60° with respect to the magnitude of the gravity vector, see Fig. 3.

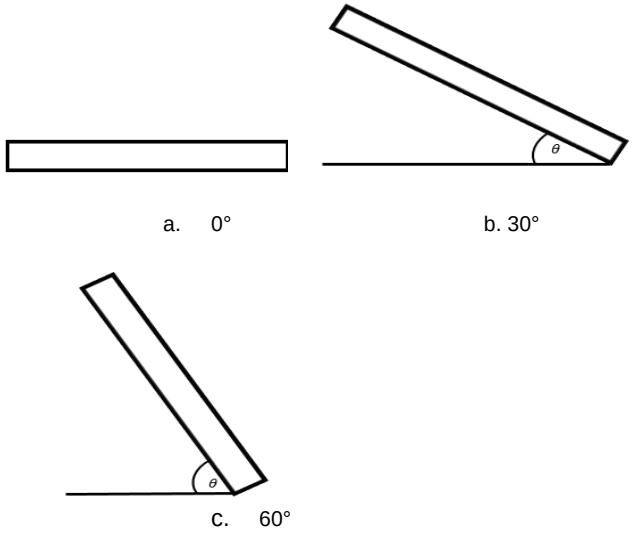

a. 0° b. 30°

c. 60°

Fig. 3.Micro-channel with smooth surface inclined at 0°, 30°, and 60°

3.2 Grid independence study

Grid independence study was performed using a microchannel of hydraulic diameter Dh=896 μm, inclined at 0°. An initial mesh dimension of 30x30, was generated, modelled and simulated to obtain the fluid flow and heat characteristics in form of the friction factor and Nusselt number, additional mesh refinements were conducted using smaller mesh dimension: 60x60, 240x240 and 360x360. The numerical solutions were compared and presented in Table 3. It is evident that there is an agreement between metrics for 240x240 and 360x360 in terms of the Nusselt number and Friction factor, because their results are nearly independent of the mesh size. In order to strike up a compromise between solution accuracy and computational time, mesh size of 240x240 was finally adopted for numerical studies.

TABLE 3: Grid independence study for microchannel fluid flow and heat transfer

Mesh Dimensions	Total elements	Nusselt number Nu	Friction factor f
30x30	11769	7.74299	0.539109
60x60	12738	7.73173	0.503907
240x240	18827	7.71248	0.465413
360x360	22555	7.70678	0.464719

4 RESULTS & DISCUSSION

The Results are divided into two major part which are: the fluid flow campaign quantified by the dimensionless friction factor, and the heat transfer campaign characterized by the dimensionless Nusselt number.

4.1 Fluid flow

The friction factor was derived using the Darcy-Weisbach equation, shown in equation 19:

$f = \frac{2D_h \Delta p}{\rho L v_{ave}^2}$ (19)

L is the channel length

g = acceleration due to gravity

ΔP = pressure difference within the channel

The friction factors were obtained from microchannels subjected to the 3 inclination angles, and plotted against the Reynolds number. The resulting effects, and phenomena for the hydraulic diameters are discussed.

Generally friction factor decreased monotonically with an increase of Reynolds number, however gravity effects were noticed at different inclination angles which varied for the respective hydraulic diameters.

Dh=199μm

As seen in Fig.4, the friction factor showed a perfect laminar behavior and decreased with a corresponding increase with the Reynolds number. The rate at which the friction factor decreased at lower Reynolds number (100-350) was steeper than for higher Reynolds number 400-950.

Friction factor for 60°, was higher than the fully developed laminar friction factor and other orientation angles.However, the margin between the inclination angles data setsreduced as the Reynolds number increased. This behavior is attributed toa growth of the velocity boundary layer thickness for 60°whichgrew thicker than those for other angles. Consequently, it acts to retard the motion of fluid particles in adjacent layer due to no-slip condition, leading to a high pressure drop and associated friction factor for lower ranged Reynolds number$Re \leq 180$.

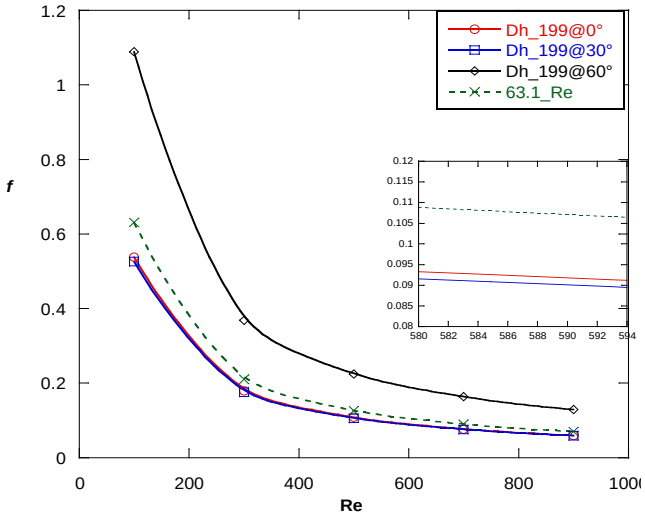

Fig. 4.Friction factor vs Reynolds number for Dh=199 μm

Dh=896μm

In Fig. 5, the Channels presented a nearly perfect laminar behavior for Dh=896μm, and the friction factors remained below the fully developed flow friction factor, with a Sharp steepness similar to Dh=199μm at lower range of Reynolds number.

The margin between the friction factor data reduced drastically, this signifies to an extent the contribution of the orientation angle towards flow optimization and pressure drop reduction.

At Re=300 an inversion process was observed, where the friction factor at 30° supersedes that of 60°.The inertia force resulting from the increasing Reynolds number acts to counteract and overcome the gravity vector, thereby diminishing gravity influence.

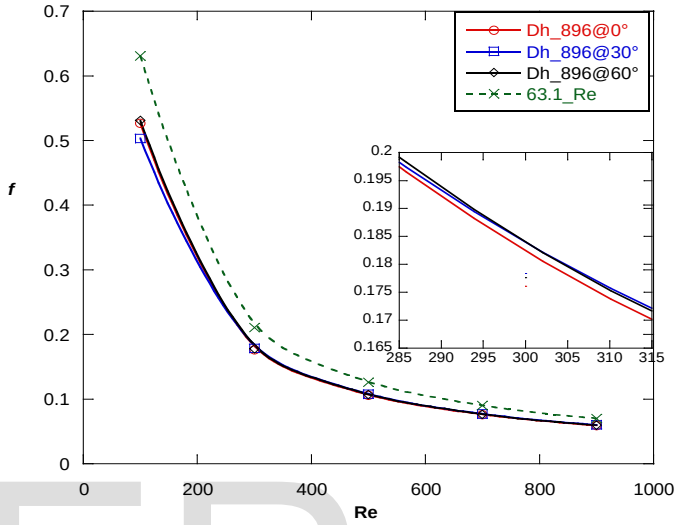

Fig. 5.Friction factor vs Reynolds number for Dh=896 μm

Dh=1587μm

Gravity effect was pronounced for Dh=1587. Friction factor for 0° was higher than 30° and 60°, as the Reynolds number increased, the margin between the data sets reduced drastically,(see Fig. 6), with this trend,gravity effect is expected to fade off around the transition zone.

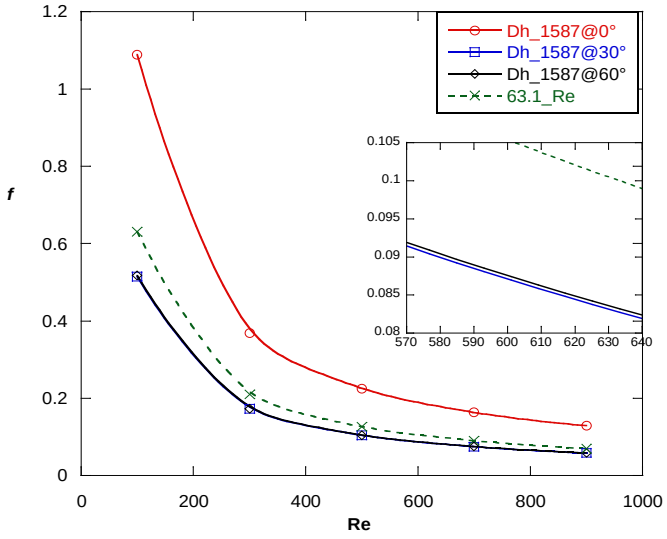

Fig. 6.Friction factor vs Reynolds number for Dh=1587 μm

4.2 Heat Transfer

The heat transfer coefficient was transformed to the dimensionless parameter Nusselt number (Nu), using the relation in equation (19).

$$Nu = \frac{h.D_h}{k} \quad (19)$$

This was done for microchannels of smooth surface, at various Reynolds number under laminar flow regime. An increase was observed for all cases, with heat transfer phenomena varying for microchannels of different hydraulic diameters, set at different orientation angles. The Nusselt number for each hydraulic diameters wasplotted against the Reynolds number, furthermore, they were compared with Nu correlations from literature.Secondly,comparisons wereconducted between the orientationanglesfor different hydraulic diameters.

Dh=199μm

Data comparison was made with experimental data from Lee et al who studied microchannels of Dh=318 μm over a range of Re from 500 to 100, there was an agreement between their data set and Nusselt for 60° over a Reynolds number range of $500 \leq Re \leq 750$(see Fig. 7). Further comparisons were made with conventional Nusselt number correlations such as results for fully developed laminar flow, Shah and londons[16], and the Sieder–Tate (SD) [16]. Data from the three inclination angles shows a general trend similar to these conventional correlations. Predictions from Stephan et al[18] agrees with Nu data for 30° and 60° at $Re \geq 1000$.

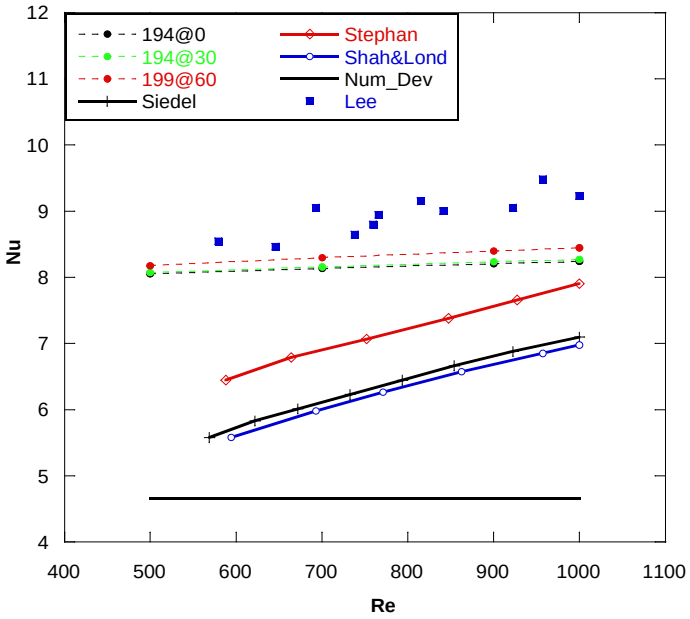

Fig. 7.Nusseltvs Reynolds number for Dh=199 μm

In Fig. 8, Nusselt numbers for each angles presented similar linear forms for microchannels of Dh =199 μm. Nusselt for 60° was the highest, and closely followed by 30°which confirms the influence of channel orientation on heat transfer between the channel wall and the coolant.

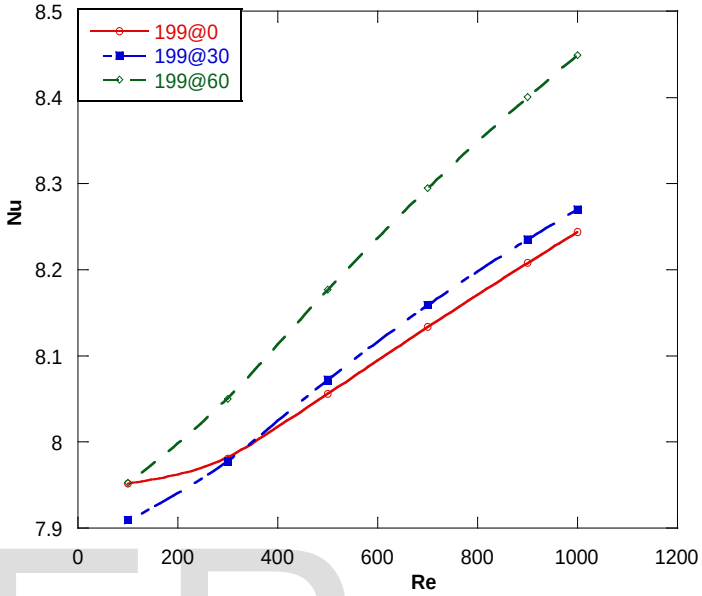

Fig. 8.Nusselt comparison for different angles with Dh=199 μm

Dh=896μm

The Nusselt numbers for microchannels for Dh=896μm are presented in Fig.9.At $Re \geq 900$, there was an agreement with Stephan-et-al, and a gradual shift from Lee et al experimental data. Generally, the data from the orientation angles presented similar characteristics as the conventional friction factor correlations which gives confidence on our results.

A zoomed image for the compared orientation anglesin Fig. 10,data revealed a change in dynamics for Dh=896μm. Firstly at $Re \leq 400$ there was a steep fall in Nu number, at Re > 400 there was a reversal and a linear increase of Nu numbers. This behavior was common to the 3 inclination angles. A likely factor responsible for this behavior is the variation in thermal lengths for the inclinationangles with respect to the Reynolds number, which increases with an increase in Reynolds number. In the same manner,the thermal boundary layer thickness varied with the Reynolds number. The thickness at Re=500 was bigger than for lower Reynolds number.

The Nusselt number for 60° was dominant at $Re < 500$, there was an inversion at Re=500, Nusselt numbers from 0° inclination dominated the other two, and 30° remained at the lowest.

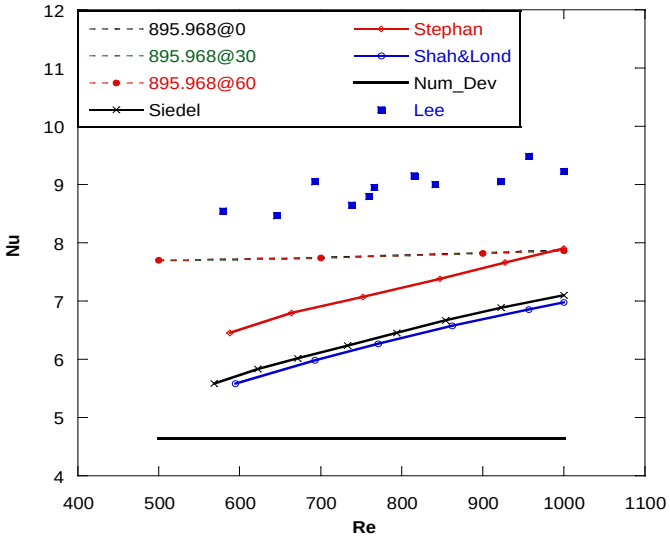

Fig. 9.Nusseltvs Reynolds number for Dh=896 μm

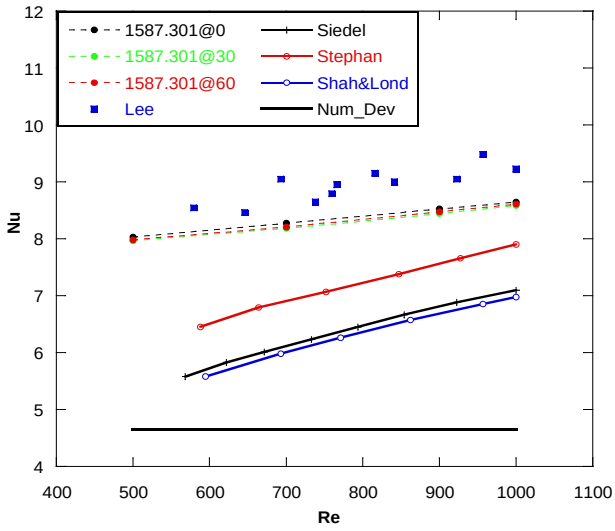

Fig. 11.Nusseltvs Reynolds number for Dh=1587 μm

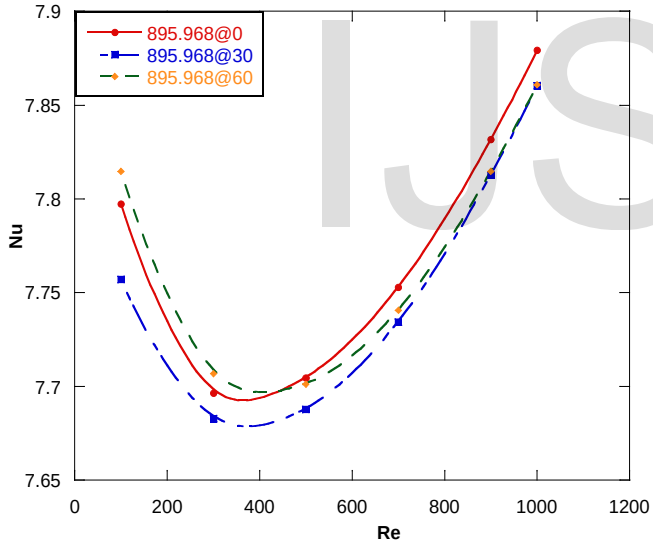

Fig. 10.Nusselt comparison for different angles with Dh=896 μm

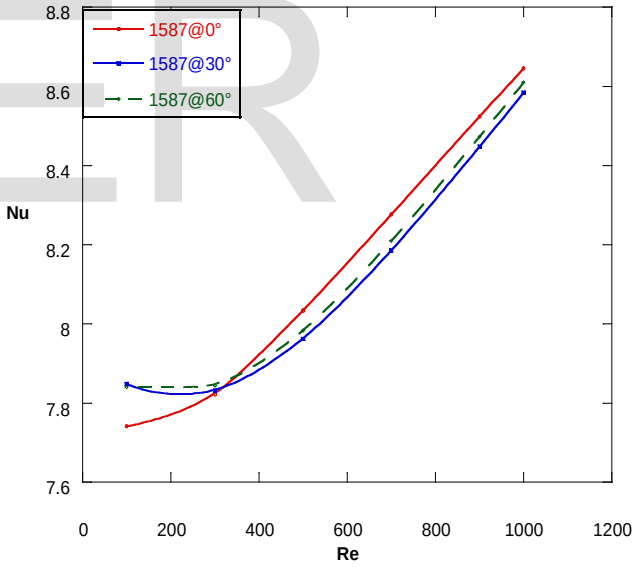

Fig. 12.Nusseltcomparison for different angles with Dh=1587μm

Dh=1587 μm

Data comparison in Fig. 11, showcased similar trends with conventional Nusselt number correlations, they gravitated closely to lee et al experimental results, and moved further away from Stephan's data. Zooming around our results in Fig. 12, revealed the dominance of 30° and 60° at $Re \leq 500$. An inversion took place at $320 \leq Re \leq 360$ and Nusselt number for 0° became higher than the others.

5 CONCLUSION

The present study assessed the effects of varying gravity conditions, in form of inclination angles on fluid flow and heat transfer capabilities, of a microchannel for single phase flow. The conclusion obtained from the study are highlighted as follows:

1. The friction factor *f*and Nusselt number (Nu) characteristics presented different behaviors for each hydraulic diameters (Dh = 199 μm, 896 μm and 1587 μm). Friction factor for Microchannel (Dh=199 μm) inclined at 60° exceeded the friction

factors for other angles at low range of Reynolds numbers $Re \leq 180$. This behavior was attributed to an increase in thickness of the velocity boundary layer which acts to retard the motion of fluid particles in adjacent layer due to no-slip condition.

2. Furthermore the gravity effect was more profound for microchannels whose hydraulic diameter ranged from$Dh \geq 1587\ \mu m$, fluid flow was largely optimized at this condition and there was a significant reduction for the pressure drop.
3. The Nusselt number was compared with experimental data from other authors and correlations from literature, excellent agreement were obtained in most cases. The gravity effect was more pronounced for Dh=199 μm, as Nusselt number for 60) was higher than the other two angles.
4. Although there exists no direct relationship between the Nusselt number and the pressure drop, we observed the existence of the heat enhancement for 60° at a cost of a high pressure drop showcased by the friction factor, this present study can be extended to establish a connecting link between the two.

ACKNOWLEDGEMENT

We would like to thank Dr. Xavier Nicolas for his useful guidance and suggestions on this work.

REFERENCE

[1] P. R. Tukermann DB, "High performance heat sinking for VLSI," *IEEE Electr Dev Lett,* vol. 2, pp. 126-129, 1981.

[2] S. G. D. L. S. C. R. M. S.G. Kandlikar, Heat transfer and fluid flow in minichannels and microchannels, Elsevier, 2014.

[3] X. T. Pega Hrnjak, "Single Phase pressure drop in microchannels," *International journal of Heat and Fluid Flow,* vol. 28, pp. 2-14, 2007.

[4] M. Omar, B. Brahim, C. Cathy and P. Hassan, "Fluid Flow and convective Heat Transfer in Flat microchannels," *International Journal of Heat and Mass Transfer,* vol. 52, pp. 1337-1352, 2009.

[5] P. C. H.Y. Wu, "Friction factors in smooth trapezoidal silicon microchannels with different aspect ratios," *International journal of heat and mass transfer,* vol. 46, pp. 2519 - 2525 , 2003.

[6] G. Gamrat, F.-. M. Michel and A. Dariusz, "Conduction and Entrance effects on laminar liquid flow and Heat transfer in Rectangular microchannels," *International journal of heat and mass transfer,* vol. 48, pp. 2943 - 2954, 2005.

[7] A. Masoud, X. Gongnan and S. Bengt, "A review of heat transfer and pressure drop characteristics of single and two-phase microchannels," *International journal of heat and Mass Transfer,* 2014.

[8] H. A. Mohammed, P. Guanasegeran and N. H. Shuaib, "Heat transfer in rectangular microchannels heat sink using nanofluids," *International communications in Heat and mass transfer,* pp. 1496 - 1503, 2010.

[9] M. R. Muhammad, "Measure of Heat Transfer in microchannel Heat sinks," *Int. comm. Heat mass Transfer,* pp. 495 - 506, 2000.

[10] W. Qu, G. M. Mala and D. Li, "Heat transfer for water flow in trapezoidal silicon microchannel," *Int. J. Heat Mass Transfer,* vol. 43, pp. 3925-3936, 2000.

[11] W. Xinyu, W. Huiying and C. Ping, "Pressure drop and Heat transfer of Al2O3-H2O nanofluids through silicon microchannels," *Journal of micromechanics and microengineering,* p. 11, 2009.

[12] W. R. Y. Xuan, "Conceptions for heat transfre correlation of nanofluids," *International journal of Heat and Mass Transfer,* vol. 43, pp. 3701-3707, 2000.

[13] Y. X. Q. Li, "Convective heat transfer and flow characteristics of Cu-water nanofluid," *Sci. China, ser,* pp. 408-416, 2002.

[14] Q. L. Y. Xuan, "Investigation on convective heat transfer and flow features of nanofluids," *ASME J. Heat Transfer,* vol. 125, pp. 151-155, 2003.

[15] Y. C. B.C. Pak, "Hydrodynamic and heat transfer study of dispersed fluids with submicron metallic oxide particles," *Exp. Heat Transfer,* vol. 11, pp. 151-170, 1998.

[16] A. L. R.K. Shah, "Laminar flow forced convection in ducts," *Adv. Heat Transfer,* vol. 1, 1978.

[17] D. D. F.P. Incropera, Fundamentals of Heat and Mass Transfer, New York: John Wiley and Sons, 1996.

[18] P. P. K. Stephan, "Wärmeübergang und maximale Wärmestromdichte beim Behältersieden binärer und ternärer Flüssigkeitsgemische," *Chemie Ingenieur Technik,* vol. 51, p. 37, 1979.